Drift waves in the corona: heating and acceleration of ions at frequencies far below the gyro frequency

J. Vranjes★ and S. Poedts†

K.U.Leuven, Center for Plasma Astrophysics, Celestijnenlaan 200B, 3001 Leuven, Belgium,
and Leuven Mathematical Modeling and Computational Science Center (LMCC)

ABSTRACT

In the solar corona, several mechanisms of the drift wave instability can make the mode growing up to amplitudes at which particle acceleration and stochastic heating by the drift wave take place. The stochastic heating, well known from laboratory plasma physics where it has been confirmed in numerous experiments, has been completely ignored in past studies of coronal heating. However, in the present study and in our very recent works it has been shown that the inhomogeneous coronal plasma is, in fact, a perfect environment for fast growing drift waves. As a matter of fact, the large growth rates are typically of the same order as the **wave** frequency. The consequent heating rates may exceed the required values for a sustained coronal heating by several orders of magnitude. Some aspects of these phenomena are investigated here. In particular the analysis of the particle dynamics within the growing wave is compared with the corresponding fluid analysis. While both of them predict the stochastic heating, the threshold for the heating obtained from the single particle analysis is higher. The explanation for this effect is given.

Key words: Sun: corona, oscillations.

1 INTRODUCTION

In our recent works Vranjes & Poedts (2009a,b,c,d) the drift wave theory has been applied to the problem of the heating of the solar corona. The drift wave is driven by gradients of the background plasma parameters (e.g., gradients of the plasma density, temperature, and magnetic field) that may act either separately or all together. In the literature, the drift wave is frequently called the *universally unstable mode* because it is growing both within the (two- or multicomponent) fluid theory and the kinetic theory. In the former (fluid) description, it is either a collisional instability (discussed in Vranjes & Poedts (2006) in the context of the solar atmosphere) that appears as a combined effect of the electron collisions, the ion inertia, and the density gradient, or a reactive one (Vranjes & Poedts 2009d) in the presence of all three gradients mentioned above where now the ions play a major role. The latter (kinetic) theory, on the other hand, can also describe these two instabilities. However, the kinetic description yields an additional (purely kinetic) instability that is absent within the fluid description. In application to the solar corona, this additional kinetic instability is studied in Vranjes & Poedts (2009a,b). This purely kinetic growth of the drift wave is entirely due to electron dynamics and it develops provided the wave frequencies are below the electron diamagnetic drift frequency.

Regardless which of the mentioned instabilities is in action, the result is always a growing wave amplitude. When some critical value for the wave potential is achieved, stochastic heating sets in (McChesney et al. 1987, 1991; Sanders et al. 1998). By nature this heating is strongly anisotropic (acting mainly in the direction perpendicular to the magnetic field vector). Moreover, it is mass dependent (heating mainly ions, with better heating of the heavier ions), it is due to the electrostatic features of the drift wave, and it is a low frequency process (typically the drift wave frequency is much below the ion gyro-frequency).

The drift wave can easily become electromagnetic in case of a relatively high plasma-β (exceeding the electron to ion mass ratio). In that limit, it is in fact coupled to the Alfvén wave. Yet, even in this case the heating develops almost without change and primarily due to the electric field of the drift-Alfvén mode. In the past, this has been studied both analytically and numerically, and it was even experimentally verified in laboratory (tokamak) plasmas (McChesney et al. 1987, 1991; Sanders et al. 1998; White et al. 2002). For the coronal environment the electromagnetic drift-Alfvén case has been discussed in detail in Vranjes & Poedts (2010).

★ E-mail: Jovo.Vranjes@wis.kuleuven.be; jvranjes@yahoo.com
† E-mail: Stefaan.Poedts@wis.kuleuven.be

For the purpose of the present study, in order to quantitatively describe some details of the heating and acceleration of plasma particles, any of the mentioned instabilities of the drift wave will do. Hence, we shall use the kinetic, density gradient driven instability from Vranjes & Poedts (2009a,b).

2   THE INSTABILITY OF THE DENSITY GRADIENT DRIVEN DRIFT WAVE

From standard textbooks (Ichimaru 1980; Weiland 2000), the frequency and the growth rate of the kinetic drift wave are given by

$$\omega_r = -\frac{\omega_{*i}\Lambda_0(b_i)}{1 - \Lambda_0(b_i) + T_i/T_e + k_y^2\lambda_{di}^2}, \tag{1}$$

and

$$\gamma \simeq -\left(\frac{\pi}{2}\right)^{1/2}\frac{\omega_r^2}{|\omega_{*i}|\Lambda_0(b_i)}\left[\frac{T_i}{T_e}\frac{\omega_r - \omega_{*e}}{|k_z|v_{Te}}\exp[-\omega_r^2/(k_z^2 v_{Te}^2)]\right.$$

$$\left.+\frac{\omega_r - \omega_{*i}}{|k_z|v_{Ti}}\exp[-\omega_r^2/(k_z^2 v_{Ti}^2)]\right]. \tag{2}$$

Here, the geometry is chosen as follows. The constant magnetic field is given by $\vec{B}_0 = B_0\vec{e}_z$, the equilibrium density gradient in the electrically neutral plasma with $n_{i0} = n_{e0} = n_0$ is given by $\nabla_\perp n_0 = -\vec{e}_x n_0' \equiv -\vec{e}_x dn_0/dx$, and the perturbations are assumed to be of the form $f(x)\exp(-i\omega t + ik_y y + ik_z z)$, with $|k_z| \ll |k_y|$ and an x-dependent wave amplitude f. The local approximation will be used. Hence, it will be assumed that $|d/dx| \ll |k_y|$.

In the derivations of Eqs. (1) and 2), the condition of a strongly magnetized plasma is used, $|\omega| \ll \Omega_i$, together with the smallness of the acoustic response of ions in the direction parallel to the magnetic field vector, implying that $\omega_r/k_z \gg c_s$, where c_s is the ion sound speed. The notation in Eqs. (1) and (2) is standard (Weiland 2000), i.e.,

$$\omega_{*e} = -k_y\frac{v_{Te}^2}{\Omega_e}\frac{n_{e0}'}{n_{e0}}, \quad \omega_{*i} = -(T_i/T_e)\omega_{*e}, \quad v_{Tj}^2 = \kappa T_j/m_j,$$

$$\Lambda_0(b_i) = I_0(b_i)\exp(-b_i), \quad b_i = k_y^2\rho_i^2, \quad \lambda_{di} = v_{Ti}/\omega_{pi},$$

where I_0 is the modified Bessel function of the first kind and of the order 0.

From Eq. (2) it is seen that within the present instability, the sign of γ can be changed only by the electron term if $|\omega_r| < |\omega_{*e}|$. This is, however, only a necessary condition. A sufficient condition is obtained when the contribution of the rest of the expression (the ion damping terms) is taken into account. As demonstrated by various graphs in Vranjes & Poedts (2009a,b), in the case of the solar corona it is more difficult to find a regime where the mode is damped than a regime where it is growing. In these studies it is shown that the mode grows more strongly for shorter perpendicular wave lengths λ_y (meter or sub-meter size) and for longer parallel wavelengths λ_z that may exceed the perpendicular ones for 4 to 5 orders of magnitude. Note that a similar ratio of the two components λ_j holds for tokamak plasmas as well. The same conclusions can also be drawn in the case of the reactive (the so-called η_i-instability) discussed in Vranjes & Poedts (2009d).

To provide some details of the particle acceleration and heating by the growing drift wave in the context of the solar corona, we need specific data. Hence, as an example we here use a set of parameters from Vranjes & Poedts (2009a,b) that are known to yield the instability: $B_0 = 10^{-2}$ T, $n_0 = 10^{15}$ m^{-3}, $L_n = [(dn_0/dx)/n_0]^{-1} = s \cdot 100$ m, $\lambda_y = 0.5$ m, and $\lambda_z = s \cdot 10^4$ m. These are just representative parameters with no particular significance. As discussed in Vranjes & Poedts (2009b), the instability will in fact develop even when the density is varied by several orders of magnitude around the given value, and the same holds for the magnetic field and the temperature. The parameter s is introduced in Vranjes & Poedts (2009a,b) for convenience only, because it was realized that the ratio γ/ω_r remains exactly the same in case the ratio λ_z/L_n is fixed. Here, L_n is the characteristic scale-length for the inhomogeneous equilibrium density. This further implies that we may go to very different scales, e.g., by taking s in the range $0.1 - 10^4$. As long as λ_y is kept constant, the ratio γ/ω_r will remain the same, although the actual values for these two quantities will certainly change. Hence, for the given parameters, from Eqs. (1) and (2) one finds $\gamma/\omega_r = 0.26$. In the case $s = 1$, this in fact implies $\omega_r = 254$ Hz and $\gamma = 66$ Hz. While in the case $s = 10^3$, this would give a mode with $\omega_r = 0.254$ Hz and $\gamma = 0.66$ Hz. Going to such small values of L_n (tens of meters) in fact makes sense because the perpendicular diffusion, that naturally develops in such a plasma with density gradients, is indeed very small, with the diffusion coefficient $D_\perp$ of the order of 0.01 m^2/s and the corresponding diffusion velocity $D_\perp\nabla_\perp n/n$ of just a few millimeters per second (Vranjes & Poedts 2008). Short values of L_n in the same time imply very high frequency drift waves and fast growing instabilities, so that the expected heating will develop at time scales that are orders of magnitude shorter than the plasma diffusion. Note that the parameters λ_z and L_n can of course also be varied independently of each other.

3   PHYSICAL MECHANISM OF HEATING BY THE DRIFT WAVE

3.1   Heating within the collective interaction frame

The physics of the mentioned stochastic heating is described in detail in various sources. Here, we give some short sketches of it by following Bellan (2006), and using the standard drift wave theory. Within the two-fluid theory, the perpendicular velocity of the ion unit volume is given by the recurrent formula (Vranjes & Poedts 2006, 2009b)

$$v_{i\perp} = \frac{1}{B_0}\vec{e}_z \times \nabla_\perp\phi + \frac{v_{Ti}^2}{\Omega_i}\vec{e}_z \times \frac{\nabla_\perp n_i}{n_i} + \vec{e}_z \times \frac{\nabla_\perp \cdot \pi_i}{m_i n_i \Omega_i}$$

$$+ \frac{1}{\Omega_i}\frac{d}{dt}\vec{e}_z \times \vec{v}_{i\perp}, \quad \frac{d}{dt} \equiv \frac{\partial}{\partial t} + \vec{v}\cdot\nabla. \tag{3}$$

The four terms here correspond to, respectively, the $\vec{E} \times \vec{B}$-drift that is usually the leading order one, the diamagnetic drift $\vec{v}_{*i}$, the stress tensor drift $\vec{v}_{\pi i}$, and the polarization drift $\vec{v}_{pi}$. The velocity can be calculated up to small terms of any order using the drift approximation $|\partial/\partial t| \ll \Omega_i$. In some situations, in plasmas with relatively cold ions, as a first approximation one may assume the $\vec{E} \times \vec{B}$-drift as the leading order one, and set it into the velocity $\vec{v}_{i\perp}$ in the polarization drift. The diamagnetic drift does not contribute

to the ion flux $\nabla \cdot (n\vec{v}_{*i}) \equiv 0$, and also its contribution to the convective derivative of the polarization drift is canceled by the part of the stress tensor flux $n\vec{v}_{\pi i}$ (Vranjes & Poedts 2009e). Therefore, we shall focus now on the $\vec{E} \times \vec{B}$-drift, and the polarization drift $\vec{v}_{pi} = (d\vec{E}_\perp/dt)/(B_0\Omega_i)$, where $\vec{E}_\perp \equiv -\vec{e}_y k_y \phi_1$. These two together describe an elliptical motion in the presence of the wave, described by:

$$\vec{v}_E = \vec{e}_x \frac{k_y \phi_1}{B_0} \sin(k_y y + k_z z - \omega_r t), \tag{4}$$

and

$$\vec{v}_{pi} = -\vec{e}_y \frac{\omega_r k_y \phi_1(t)}{B_0 \Omega_i} \left[\left(1 - \frac{k_z}{\omega_r}\frac{dz}{dt}\right)\cos\varphi - \frac{\gamma}{\omega_r}\sin\varphi \right] \times$$

$$\times 1/\left(1 - \frac{k_y^2 \phi_1(t)}{B_0 \Omega_i}\cos\varphi\right), \quad \varphi = k_y y + k_z z - \omega_r t. \tag{5}$$

In deriving Eq. (5) the wave amplitude is taken as time dependent due to the wave instability, $\phi_1 = \widehat{\phi}\exp(\gamma t)$, $\widehat{\phi} = \mathrm{const.}$, and the same holds for the coordinates $y(t), z(t)$ appearing in the wave phase $\varphi(t)$. That is the reason for the appearance of the terms with γ and dz/dt. Neglecting these two terms, and taking a constant potential, Eq. (5) becomes identical to the corresponding expression from Bellan (2006).

Crucial for the heating is the term $[k_y^2 \phi_1(t)/(B_0\Omega_i)]\cos\varphi$ in the denominator. Looking back into the derivations, it turns out that it appears from the derivative $d(\sin\varphi)/dt \rightarrow dy/dt = v_y = v_{pi}$. Keeping it here has sense only in case of a relatively large displacement in the direction of the perpendicular wave vector. From Eq. (5) it is seen that for

$$a(t) \equiv k_y^2 \phi_1(t)/(B_0\Omega_i) = k_y^2 \rho_i^2 e\phi_1(t)/(\kappa T_i) \geqslant 1, \tag{6}$$

the denominator may vanish and, consequently, the polarization drift should go to infinity. Note however, that Eq. (5) is obtained approximately starting from the guiding center approximation that becomes violated for such a large polarization drift, and the analytical expression for the polarization drift in this limit becomes inaccurate. Yet, Eq. (5) describes the general trend for the polarization drift; a fast and significant acceleration and heating of the plasma particles will definitely take place, as experimentally verified in McChesney et al. (1987, 1991); Sanders et al. (1998).

3.2   Individual particle dynamics

As discussed in Bellan (2006), a direct numerical integration for plasma particles is required for a full validation of the above described heating mechanism for the solar corona. The numerical simulation has to take into account the actual values of the electric field in the position of a specific gyrating plasma particle. For that purpose, taking again the drift-wave electric field with a time-varying amplitude, the appropriate set of equations for a single particle reads

$$y''(t) + y(t) - a(t)\sin\left[y(t) + \frac{k_z}{k_y}z(t) - bt\right] = 0, \tag{7}$$

$$z''(t) - a(t)\frac{k_z}{k_y}\sin\left[y(t) + \frac{k_z}{k_y}z(t) - bt\right] = 0, \tag{8}$$
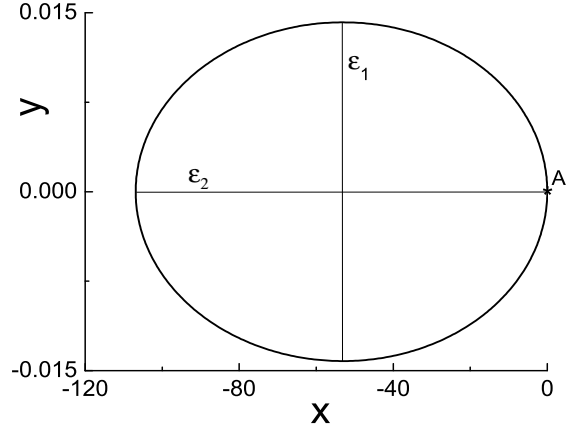
$$x'(t) - y(t) = 0. \tag{9}$$

Figure 1. Particle positions in the x, y-plane within a wave period, after it starts from the point A with $(x, y, z) = (0, 0, 0)$, for a small wave amplitude $\phi_1 = 0.86$ V.
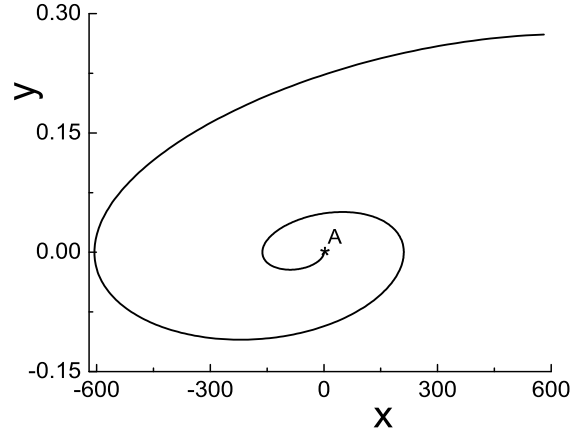

Figure 2. Normalized particle positions in the x, y-plane after it starts from the point A with $(x, y, z) = (0, 0, 0)$, for a growing electric field potential $\phi_1(t) = \widehat{\phi}\exp(\gamma t/\Omega_i)$, and $\widehat{\phi} = 0.86$ V.

Here, the prime denotes a derivative in time, and the spatial and time coordinates are normalized as $x, y, z \rightarrow k_y x, k_y y, k_y z$, $t \rightarrow \Omega_i t$, $b = \omega_r/\Omega_i$. Equation (9) is obtained after one integration where an integration constant appears that has been neglected. Note that Eq. (7) can be reduced to the Mathieu equation with a source term. Namely, neglecting the z-terms and after introducing $\tau = bt/2$, for the small remaining argument φ it can be written in the generic form

$$d^2y/d\tau^2 + [\alpha - 2q(t)\cos 2\tau]y(\tau) = c(\tau)\sin 2\tau, \tag{10}$$

where $\alpha = 4/b^2$, $q(\tau) = 2\alpha(\tau)/b^2$, and $c(\tau) = -4\alpha(\tau)/b^2$. The solutions of this equation without the right-hand side are the Mathieu functions $M(\alpha, q, \tau)$. Equation (10) has unstable solutions and it is discussed in detail in **?,** White et al. (2002).

The set of ordinary equations (7)-(9) is solved numerically. We do this first for a very small and constant wave amplitude in order to demonstrate some basic features of the particle motion due to the wave electric field. The result
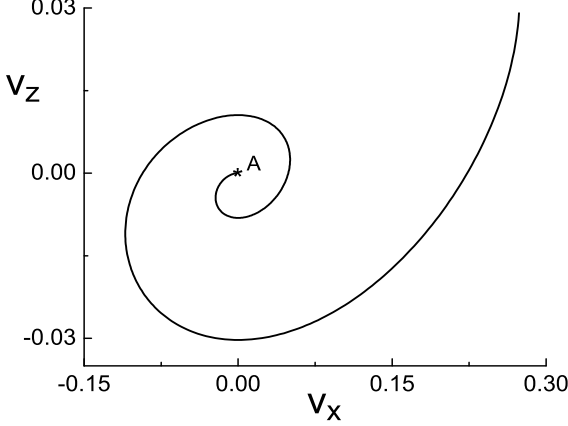
Figure 3. Normalized velocities v_x, v_z for the same parameters as in Fig. 2.
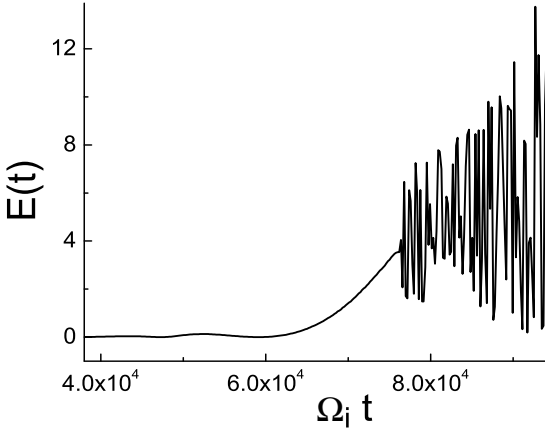

Figure 4. Change in time of the normalized kinetic energy of a particle with a unit mass $E = (v_x^2 + v_y^2 + v_z^2)/2$.

is shown in Fig. 1, where we give the projection of the proton positions in the perpendicular plane, $x(t), y(t)$, in the wave field with the constant amplitude $e\phi_1/(\kappa T_i) = 0.01$, that corresponds to $\phi_1 = 0.86$ V. Here and further in the text we take $\lambda_y = 0.5$ m, $\lambda_z = 2 \cdot 10^4$ m, which consequently from Eq. (1) yields the wave frequency $\omega_r = 254$ Hz. The normalization is the same as above, viz. $(x, y) \equiv (k_y x, k_y y)$. This all yields $a = 0.014$, hence the stochastic heating is absent, and the particle trajectory is a very elongated ellipse, with the motion almost completely in the x-direction due to the $\vec{E} \times \vec{B}$-drift described above (observe the difference in x, y-scales). After a wave period the particle returns to the starting position A with the coordinates $(x, y) = (0, 0)$. The ratio of the two axes of the ellipse $\varepsilon_1/\varepsilon_2 = 0.00013$ describes the fact that the particle motion is mainly due to the $\vec{E} \times \vec{B}$-drift in the x-direction, and that the polarization drift in the direction of the wave-vector (the y-direction) is negligible.

Performing the same plot for electrons yields the same ϵ_2 as expected (the $\vec{E} \times \vec{B}$-drift is independent on mass), while ϵ_1 becomes reduced by the factor m_e/m_i (the polarization drift separates charges and it is mass dependent).

On the other hand, taking a time-varying potential $\phi_1(t)$ due to the above demonstrated drift wave instability, and restricting the time interval to relatively short values (below the onset time of the stochastic heating), yields a spiral trajectory in the x, y-plane. One example of this is presented in Fig. 2. Here, the starting value for the potential is the same as above $e\phi_1(0)/(\kappa T_i) = 0.01$, and the same holds for the particle position. The other parameters are the same as in Fig. 1. With the same normalization the potential is given by $\phi_1(t) = \widehat{\phi} \exp(\gamma t/\Omega_i)$, $\gamma = 0.26\omega_r$, $\omega_r = 254$ Hz, $\widehat{\phi} = \phi_1(0)$. The maximum time in physical units here is 0.04 s, and in this moment the potential has reached the value of 17 V. Comparing with Fig. 1, one observes that the displacement in the y-direction due to the polarization drift is now increased by a factor 20.

It is interesting to compare the leading perpendicular $\vec{E} \times \vec{B}$-drift velocity v_x, and the parallel velocity v_z (along the magnetic field vector). The parametric plot in Fig. 3 shows that for these potential amplitudes the parallel velocity v_z remains about one order of magnitude smaller.

In order to see what happens for larger amplitudes of the electrostatic drift wave when the stochastic heating is supposed to be in action, Eqs. (7)-(9) are solved by allowing a slightly larger time range. One of the results is shown in Fig. 4 for the kinetic energy of a particle with unit mass $E(t)/m = [v_x(t)^2 + v_y(t)^2 + v_z(t)^2]/2$, with normalized velocities as above. The other parameters are the same as in the previous text and figures. Here, the stochastic heating takes place after around 0.078 s, in the moment when the growing wave amplitude reaches the value of around 150 V. Note that this is by about a factor 2.5 larger than the value obtained from the condition (6) which, in fact, follows from an approximative procedure as explained earlier. Thus, a higher necessary threshold for the stochastic heating is expected. However, a plasma can support multiple waves in the same time. The drift wave spectrum described by Eqs. (1, 2) in realistic situations imply the presence of more waves rather than a single one. The analysis presented in a recent study (Sheng et al. 2009) shows that in such cases the instability threshold can be considerably reduced. Therefore, the ion heating by the mechanism which we discuss here will be even more efficient.

The corresponding plot of the displacement in the direction of the wave $y(t)$, which is in fact also equal to the velocity $v_x(t)$ [see Eq. (9)] is shown in Fig. 5. The plot of the velocity $v_y(t)$ (that is not given here) reveals the amplitude that is completely negligible until $\Omega_i t$ becomes close to $8 \cdot 10^4$; after that it is very stochastic and with the amplitude equal to that of the velocity $v_x(t)$. Thus we are in the range of parameters in which the expansion procedure used previously is not valid any longer because the polarization and $\vec{E} \times \vec{B}$ drifts are of the same order, and the stochastic heating is fully in action. Note that, although the motion is stochastic/chaotic, it is in fact deterministic and not random as commented in Bellan (2006). Observe that the total physical time interval for Figs. 4 and 5 is only about 3-4 wave-periods.

The plot of the parallel velocity $v_z(t)$, presented in Fig. 6, shows that along the magnetic field the particle dynamics remains non-stochastic, as should be expected in view of the analysis presented in the text above. The velocity magnitude is below 1, thus still smaller than the per-
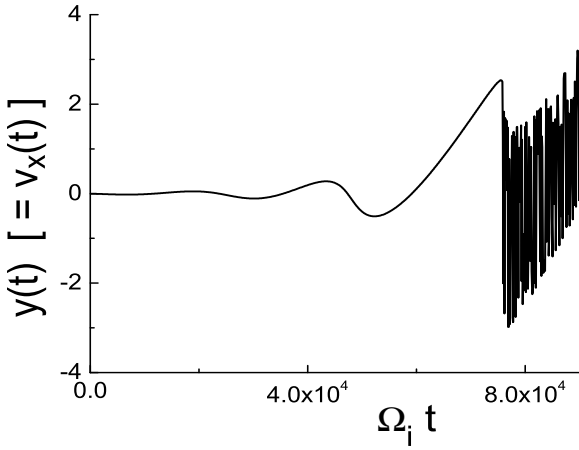
Figure 5. Normalized displacement in the direction of the polarization drift $y(t)$, and the normalized perpendicular velocity component $y(t) \equiv v_x(t)$.
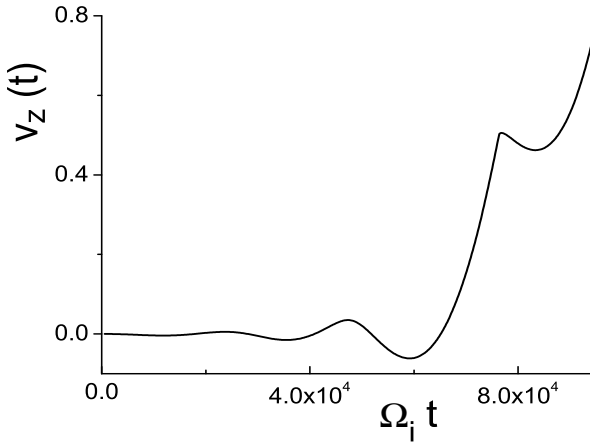

Figure 6. Normalized perturbed velocity in the direction parallel to the magnetic field.

pendicular velocity (see Fig. 5) which is the consequence of the stochastic heating.

The theory presented in McChesney et al. (1987, 1991); Sanders et al. (1998) predicts the maximum stochastic velocity $v_{max} \simeq [k_y^2 \rho_i^2 e\phi/(\kappa T_i) + 1.9]\Omega_i/k_y$, which further yields the effective achieved stochastic temperature $T_{max} = mv_{max}^2/(3\kappa)$. For the parameters used above this yields $T_{max} \simeq 2 \cdot 10^6$ K, i.e., the increase of the temperature for one million Kelvin within the growth time $\tau_g \simeq 0.1$ s. The maximum energy released by this mechanism is $\Sigma_{max} = n_0 m_i v_{max}^2 = 0.04$ J/m^{-3}. The energy release rate, Σ_{max}/τ_g, exceeds for several orders of magnitude (Vranjes & Poedts 2009a,b) the value presently accepted by researchers as required for a sustained coronal heating.

4 SUMMARY

The present study provides some additional details of our recently proposed model for the coronal heating, which implies the heating by electrostatic drift waves. The heating by waves, which presently represents one of two ma-

jor heating scenarios, has been studied in many works from the early days of the coronal heating investigation, e.g., by Alfvén (1947) and Piddington (1956), but also more recently in Pekünlü et al. (2001); Suzuki (2004). More details about the existing heating models are available in various sources (Narain & Umschneider 1990; Klimtchuk 2006), some of them have also been discussed in more detail in our recent work Vranjes & Poedts (2009b).

In this work, the trajectories of individual plasma particles have been investigated within the framework of the drift wave instability and the associated stochastic heating, with the aim to describe some fine details of the particle dynamics during the heating process. The calculation of the actual growth rates of the mode is not repeated here because it has been given in detail in our recent studies. From the present study and from our recent works it follows that the general trend of the ion behavior in the wave field with a growing amplitude can be described analytically from the fluid point of view, as discussed here in Sec. 3.1. However, a more detailed picture is obtained by following a single particle which is moving in the wave field. For example, this is seen from Sec. 3.2 in the case of the critical threshold for the onset of the heating. We observe that the general theory of the drift wave instability presented in some early studies (Terashima 1967), and not necessarily related to the heating, also includes the particle aspect approach, and as such, is in perfect agreement with the fluid and kinetic modeling.

It is also interesting to note that, although the individual particle dynamics becomes stochastic for relatively large wave amplitudes, the overall picture of the macroscopic motion of the plasma, caused by the wave, actually remains well described by the fluid description. This has been directly experimentally verified by Bailey et al. (1993). The parameter a [c.f. Eq. (6)] in their experiment was around 2, and thus the stochastic heating was in action, yet the observed electrostatic potential and density profiles nicely matched the theoretical contour plots corresponding to a wave described within the fluid theory and drift approximation. This is in agreement with the statement given in Sec. 3.2 about the nature of the heating; the increased effective temperature T_{max} follows from the stochastic velocity v_{max} which in fact is not random, yet in practical terms it is indistinguishable from standard collisional thermalization and the broadening of the distribution function (Bellan 2006).

The model used here implies a maxwellian distribution function for plasma species, that is the basis for both the kinetic and the fluid description of the instability. However, the stochastic heating with all its features (Vranjes & Poedts 2009b,d) in fact implies that such a starting distribution function will necessarily evolve. The perpendicular ion temperature will grow and eventually become larger than the parallel one. Hence, the particle distribution may pass through several stages, going through the Oort's distribution with the temperature anisotropy and to the more general loss-cone distribution (Baronia & Tiwari 1999), or to something else. This opens an interesting possibility for eventual numerical simulations because such fine details are beyond the scope of an analytical study.

ACKNOWLEDGMENTS

REFERENCES

Alfvén, H., 1947, MNRAS, 107, 211
Bailey, A. D., Stern, R. A., Bellan, P. M., 1993, Phys. Rev. Lett., 71, 3123
Baronia, A., Tiwari, M. S., 1999, Planet. Space Sci., 47, 1111
Bellan, P. M., 2006, Fundamentals of Plasma Physics. Cambridge Univ. Press, Cambridge, p. 106
Ichimaru, S., 1980, Basic Principles of Plasma Physics. The Benjamin/Cummings Publish. Comp., Reading, Massachusetts
Narain, U., Ulmschneider, P., 1990, Space Sci. Rev., 54, 377
Klimtchuk, J. A., 2006, Solar Phys., 234, 41
McChesney, J. M., Stern, R. A., Bellan, P. M., 1987, Phys. Rev. Lett., 59, 1436
McChesney, J. M., Bellan, P. M., Stern, R. A., 1987, Phys. Fluids , 59, 1436
Pekünlü, E. R., Çakirli, Ö., Özetken, E., 2001, MNRAS, 326, 675
Piddington, J. H., 1956, MNRAS, 116, 314
Sanders, S. J., Bellan, P. M., Stern, R. A., 1998, Phys. Plasmas, 5, 716
Sheng, Z. M., Yu, L., Hao, G., White, R., 2009, Phys. Plasmas, 16, 072106
Suzuki, T. K., 2004, MNRAS, 349, 1227
Terashima, Y., 1967, Prog. Theor. Phys., 37, 775
Vranjes, J., Poedts, S., 2006, A&A, 458, 635
Vranjes, J., Poedts, S., 2008, A&A, 482, 653
Vranjes, J., Poedts, S., 2009a, EPL, 86, 39001
Vranjes, J., Poedts, S., 2009b, MNRAS, 398, 918
Vranjes, J., Poedts, S., 2009c, Phys. Plasmas, 16, 092902
Vranjes, J., Poedts, S., 2009d, MNRAS, 400, 2147
Vranjes, J., Poedts, S., 2009e, A&A, 503, 591
Vranjes, J., 2010, ApJ, to be published
Weiland, J., 2000, Collective Modes in Inhomogeneous Plasmas. Institute of Physics Pub., Bristol
White, R., Chen, L., Lin, Z., 2002, Phys. Plasmas, 9, 1890

This paper has been typeset from a TEX/ LATEX file prepared by the author.